Trends and prediction of extreme precipitation indices in three cities of Burkina Faso using non-parametric statistics and the Holt-Winters smoothing method

Joseph Yaméogo [ID]

Ziniaré University Center/Joseph Ki-Zerbo University, Burkina Faso

Abstract

Climate extremes have become increasingly important in recent years, leading to renewed scientific interest. However, few studies have focused on precipitation extremes in cities in Burkina Faso, a Sahelian country in West Africa. The aim of this study is to analyze trends and to project future extreme precipitation indices in three cities in Burkina Faso. To this end, precipitation data, recorded daily, were collected from the National Meteorological Agency of Burkina Faso (NMABF) over the period 1991-2020. The stations selected were Boromo for the small town of Boromo, Saria for the medium-sized town of Koudougou, and Bobo-Dioulasso for the town of Bobo-Dioulasso. The precipitation data were used to calculate the extreme precipitation indices described by ETCCDMI (Expert Team for Climate Change Detection Monitoring and Indices) using Rclimdex. Descriptive statistics, the Mann-Kendall test, and trends from innovative models were used to analyze the extreme precipitation indices; the Holt-Winters additive model was used to analyze future projections. The study showed considerable variability and a monotonic increasing trend in extreme precipitation indices over the period 1991-2020. However, for the city of Koudougou, the trend was a non-monotonic increase. The forecast based on the Holt-Winters additive model shows considerable variability in the extreme precipitation indices, with an upward trend over the period 2020-2030. On the other hand, in the city of Koudougou, indices of precipitation duration will decrease, indicating that the city will be affected most by the frequency and intensity of extreme precipitation.

1. Introduction

Fluctuations in temperature and precipitation are widely recognized as relevant indicators of global climate change and variability (IPCC 2021). Anthropogenic activities that increase greenhouse gases cause temperature increases and regional changes in mean climate, resulting in climate extremes in various parts of the world (IPCC 2023). In West Africa, several studies, including in Nigeria (Gbode et al. 2019), Mauritania, Guinea, Côte d'Ivoire, Senegal, Mali, and Niger (Barry et al. 2018), have observed these changes. Sylla et al. (2015) add that the increase in the intensity of very wet events, particularly in the pre- and early monsoonal periods, will be more marked over the Sahel and under Representative Concentration Pathway (RCP) 8.5 than in the Gulf of Guinea under RCP 4.5. Urban areas will also be affected by climate extremes in West Africa (Herslund et al. 2015), which is a major concern.

African cities are experiencing an unprecedented increase in the rate of urbanization. Between 1990 and 2022, 500 million people are expected to move to urban centers in Africa (OECD 2022). By 2050, Africa's urban population is expected to reach 1.06 billion (Ezeh et al. 2020). This demographic growth will increase the impact of climate extremes on urban populations. Extreme precipitation caused flooding in Dar es Salaam on 22 December 2011, resulting in 20 deaths, extensive damage, and loss of livelihoods

(Giugni et al. 2015). The same happened in Lagos, Nigeria (Doan et al. 2023) and Dakar, Senegal (Diémé et al. 2025). In Burkina Faso, the situation is no better than in other West African countries. The country is experiencing an increase in precipitation and extreme temperature indices in the north, Boucle du Mouhoun, and southwest regions (Rouamba et al. 2023; Yaméogo, Rouamba 2023a; Yanogo, Yaméogo 2023; Yaméogo 2024; Yaméogo, Sawadogo 2024; Yaméogo 2025), with dramatic consequences for the population (Yaméogo, Rouamba 2023b). In this context, (Gimeno et al. 2022) note that the increase in urban populations associated with climate change makes societies increasingly vulnerable to extreme precipitation.

A few studies have examined extreme precipitation trends and projections. For example, the work of Rouamba et al. (2023) in the municipality of Boromo, in the south of Burkina Faso (Sougué et al. 2023), and in ten cities in Burkina Faso addressed the issue of trends and forecasts of climatic extremes in recent years. Several statistical methods, especially approaches based on the classical theory of extremes (peak-on-threshold) and linear regression models, have been used by various authors to understand the spatiotemporal trends in climate extremes (Béwentaoré, Barro 2022; Rouamba et al. 2023). Parametric regression models have also been used to predict future extreme events using CMIP6 data (Koala et al. 2023). These studies do not account for trends and seasonality of the time series of climate extremes, which can bias trends and forecasts of precipitation extremes.

Several other advanced forecasting methods are reported in the literature, including the Holt-Winters smoothing method, which accounts for trend and seasonality (Nurhamidah et al. 2020). This method has advantages, such as reducing the weight of historical data, and simplicity. Therefore, it has been used in several studies in the field of climatology (Gundalia, Dholakia 2012; Gowri et al. 2022; Bhagat, Ramaswamy 2023). This prediction method can make valuable contributions to understanding future trends and impacts of climate change (Pala, Şevgin 2024). The method thus forms the basis of statistical modeling for climate prediction in the region. The general objective of this study is to analyze the evolution of extreme precipitation indices and their projection from 2020 to 2030 using non-parametric smoothing and Holt-Winters methods in three cities in Burkina Faso. The secondary objectives of this study are to:

- analyze the variability of extreme precipitation indices over the period 1991-2020;
- analyze the trends in extreme precipitation indices over the period 1991-2020;
- determine the projection of extreme precipitation indices for the period 2020-2030.

2. Materials and methods

2.1. Study area

The study areas are in Burkina Faso, West Africa (Fig. 1). Three cities are considered in the study: Bobo-Dioulasso, in the urban commune of the Houet province in the Hauts Bassins region. These cities vary in physical characteristics. The soils of Koudougou, Burkina Faso, are varied. They include leached tropical ferruginous soils, often poor in organic matter and nutrients, and lithosols on cuirass, better suited to

grazing. Hydromorphic soils are also found along watercourses, which are favorable to certain crops. The area is affected by soil degradation, with a widening of the Sahel and a decline in vegetation. The soils in Boromo, Burkina Faso, are diverse and include cuirass, hydromorphic, and tropical ferruginous soils. These soils have various properties influenced by their origin and environment. Some are suitable for agriculture, while others are susceptible to erosion. The soils of Bobo-Dioulasso, Burkina Faso, are mainly characterized by ferralitic soils, tropical ferruginous soils, and eutrophic brown soils. These soils result from weathering of Birrimian rocks and vary according to relief and topography. In human terms, the study towns have different populations. Bobo-Dioulasso is the second-largest city in Burkina Faso, covering an area of 1,805 km². Its population is >900,000. Koudougou is a medium-sized town, Burkina Faso's third-largest city. Its population has been particularly dynamic in recent decades. Its urban population has more than quadrupled over the past few decades, from 36,838 in 1975 to 88,184 in 2006 and 160,239 in 2019 (Sirven 1987; INSD 2011). Boromo is one of the country's smaller towns. Its urban population is estimated at 20,193 (INSD 2011). Unlike other towns, Boromo is facing an influx of people fleeing terrorism in the north of the country. This situation makes the small town of Boromo vulnerable and exacerbates social problems (Yaméogo et al. 2022).

These three towns were selected based on three criteria: the availability of rainfall data over a given period, the degree of missing data over a given period, and the size of the population potentially affected by extreme rainfall. The populations of these towns have increased considerably as a result of the security crisis in the northern, eastern, and Boucle du Mouhoun areas.

The topography varies throughout the region. The towns studied have altitudes ranging from 232 to 314 to >478 m (Fig. 2).
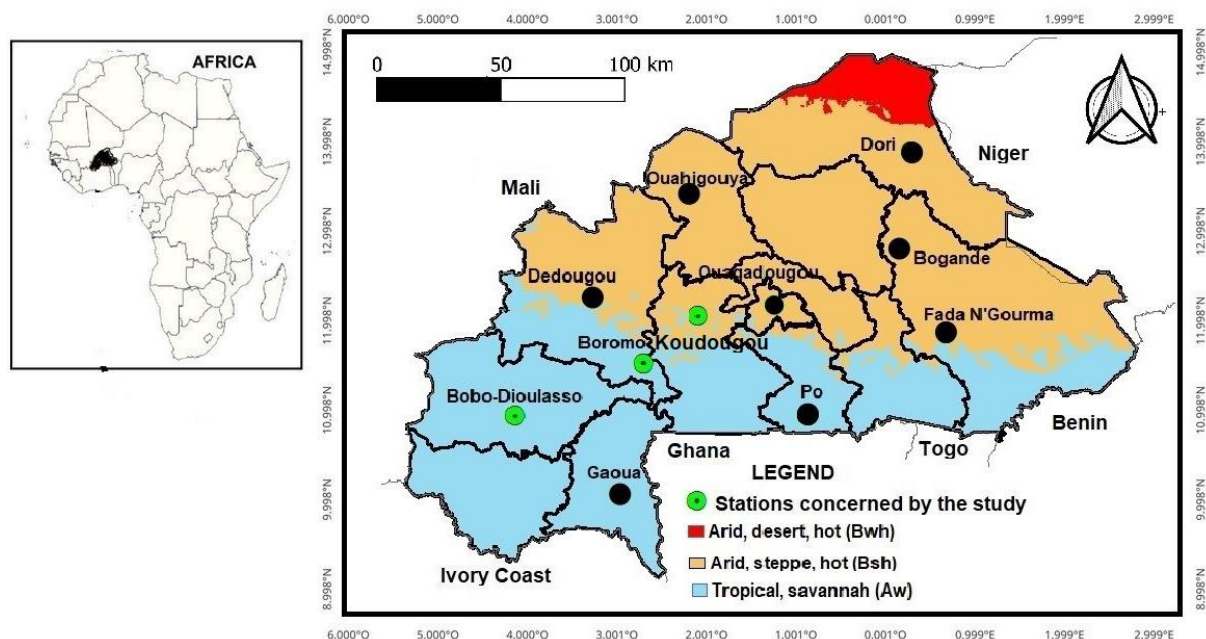

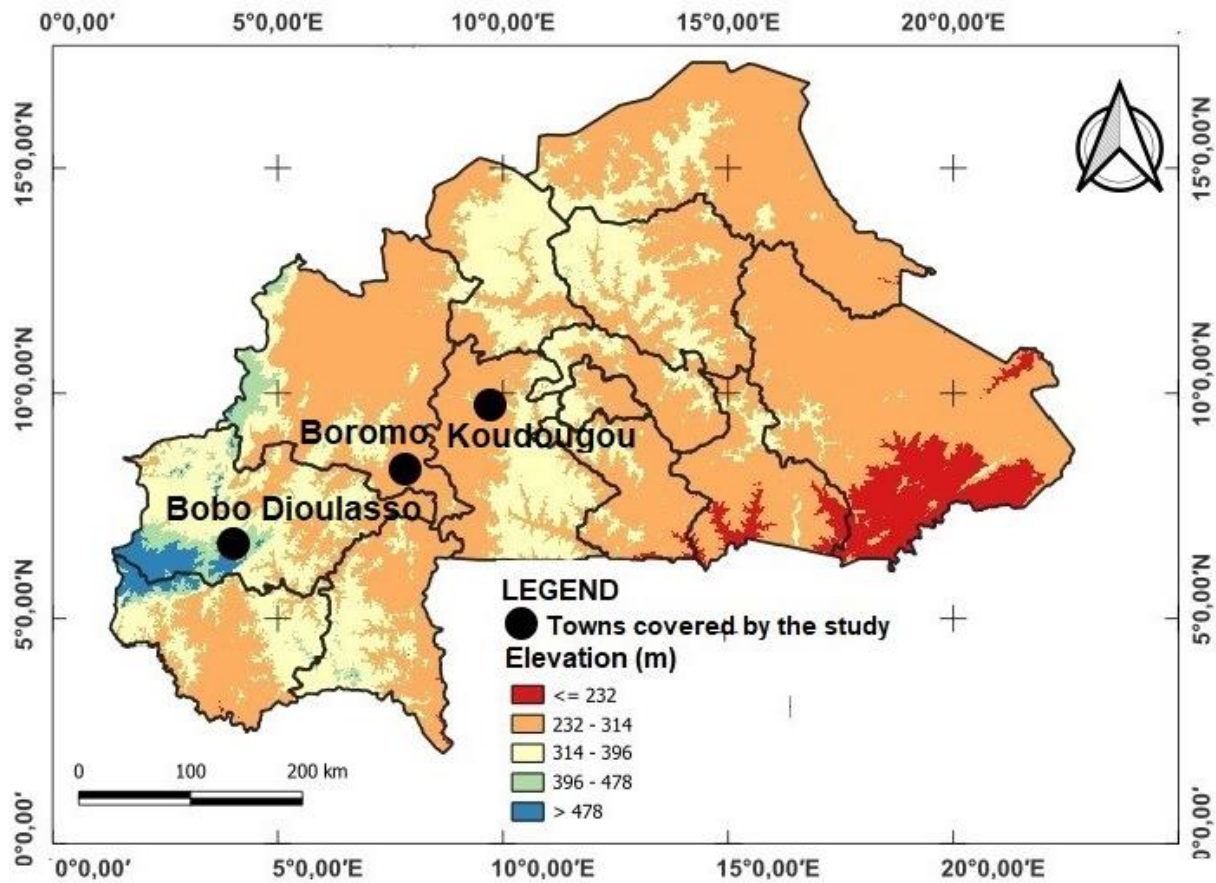Fig. 1. Geographical location of study towns and stations.

Fig. 2. The topography of Burkina Faso.

2.2. Data and methods

Daily precipitation data were obtained from the National Meteorological Agency of Burkina Faso for 1991-2020 (Table 1). One station was selected for each of the three towns. The Saria station represents the town of Koudougou, the Boromo station the city of Boromo, and the Bobo-Dioulasso station the city of Bobo-Dioulasso.

Table 1. Characteristics of the selected stations

Station names	Type of station selected	Type of domain climate	Period selected	Latitude (N)	Longitude (E)
Bobo-Dioulasso	Synoptic station	Sudanian	1991-2020	11.1667	–4.3167
Boromo	Synoptic station	Sudano-sahelian	1991-2020	11.75	–2.9333
Saria	Climatological station	Sudano-sahelian	1991-2018	12.2667	–2.15

Daily precipitation data were fed into Rclimdex, which produced extreme precipitation indices for the period 1991-2020, representing precipitation intensity, precipitation frequency, and precipitation duration. RClimDex provides a user-friendly graphical interface for calculating the 27 basic indices recommended by the CCl/CLIVAR Expert Team on Climate Change Detection, Monitoring and Indices (ETCCDMI) (Karl et al. 1999; Zhang, Yang 2004). In the present study, 10 indices were selected (Table 2).

Table 2. Extreme precipitation indices used in the study. Source: Lourdes et al. (2021).

Index classification	Index	Description	Unit
Intensity indices precipitation	Rx1day	Maximum precipitation over 1 day	mm
	Rx5day	Maximum consecutive precipitation over 5 days	mm
	SDII	Annual total precipitation divided by the number of wet day	mm/day
	prpcptot	Total precipitation in wet days ≥ 1 mm	mm
Frequency indices precipitation	R99ptot	Number of days with precipitation ≥ 99th percentile	day
	R95ptot	Number of days with precipitation ≥ 95th percentile	day
	R10mm	Number of days precipitation ≥ 10 mm	day
	R20mm	Number of days precipitation ≥ 20 mm	day
Duration indices precipitation	CDD	Maximum number of consecutive days with precipitation < 1 mm	day
	CWD	Maximum number of consecutive days with precipitation ≥ 1 mm	day

The data projections for the 10-year period (2020-2030) were based on the extreme precipitation indices extracted from the daily data using Rclimdex. The temporal data for the extreme precipitation indices were processed in XLSTAT 2019 using the Holt-Winters method.

2.2.1. Mann-Kendall Test

It is a non-parametric test and there is no requirement that the data must be normally distributed (Oufrigh et al. 2023). In this test, H_0 is the null hypothesis, which states that the data come from a population whose observations are independent of each other and are uniformly distributed, and the alternative to H_1, which states that the data have a monotone tendency (Aditya et al. 2021). These test values $(Xj - Xk)$ where $j > k$ and the test statistic S is calculated by applying the formula (Shah, Kiran 2021):

$$S = \sum_{k=1}^{n-1} \sum_{j=k+1}^{n} sgn(Xj - Xk) \tag{1}$$

With, Xj and Xk are the annual values for years j and k, $j > k$, respectively.

The *sgn* function is calculated as follows:

$$sgn(Xj - Xk) = \begin{cases} 1 \ if \ Xj - Xk > 0 \\ 0 \ if \ Xj - Xk = 0 \\ -1 \ if \ Xj - Xk < 0 \end{cases} \tag{2}$$

The test statistic, τ, can be calculated as follows:

$$\tau = \frac{s}{n - \dfrac{(n-1)}{z}} \tag{3}$$

In order to statistically quantify the significance of the trend, it is necessary to calculate the probability associated with S and the sample size n. The formula to calculate the variance S is as follows:

$$Var(S) = \frac{1}{18}\left[n(n-1)(2n+5) - \sum_{i=1}^{m}(t_i-1)(2t_i+5)\right] \tag{4}$$

Where q is defined as the number of linked groups and t_p is defined as the number of data items in the pth group. The values of S and $Var(S)$ are used for the calculation of the test statistic Z, which is:

$$Z = \begin{cases} \dfrac{s-1}{\sqrt{Var(s)}}, & if\ s > 0 \\ 0 & if\ s = 0 \\ \dfrac{s+1}{\sqrt{Var(s)}}, & if\ s < 0 \end{cases} \tag{5}$$

The null hypothesis h_0 (no trend) is rejected if the significance level or p-value is >5%.

2.2.2. Innovative trend analysis method (ITAM)

This technique, introduced by Şen (2017), or referred to as new trend analysis (Sezen, Partal 2020), is non-parametric and its use does not require a normal distribution of observations (Şen et al. 2019; Mallick et al. 2021). It is a very useful tool for detecting trends in precipitation time series data (Pastagia, Mehta 2022; Patel, Mehta 2023). In addition, the ITAM is more sensitive in determining the trend than the Mann-Kendall (MK) test (Mohorji et al. 2017; Sanusi, Abdy 2021; Kessabi et al. 2024). In ITAM, the data series is divided into two equal parts such that (Dabanlı et al. 2016; Mohorji et al. 2017; Şen et al. 2019; Marak et al. 2020; Kougbeagbede 2024; Muthiah et al. 2024).

Mathematically, the procedure of the method is translated as follows (Güçlü 2020):

- Any data consisting of n data, $a_1, a_2, ..., a_n$ is separated into two equal series $\{b_{1,\ n/2}\}$ and $\{b_{2,\ n/2}\}$, such as:

$$\{b_{1,\ n/2}\} = \{a_1, a_2, ..., a_{n/2}\} \tag{6}$$

and

$$\{b_{2,\ n/2}\} = \{a_{n/2+1} + a_{n/2+2}, ..., a_n\} \tag{7}$$

- Each series with the same number of elements is then listed in ascending order. The series is named as follows: $\{S_1\}$, et $\{S_2\}$, with:

$$\{S_1\} = \{\min(b_{1,\ n/2}), ..., b_j, ..., \max(b_{1,\ n/2})\}\ (1<i<n/2) \tag{8}$$

and

$$\{S_2\} = \{\min(b_{2,\ n/2}), ..., b_j, ..., \max(b_{2,\ n/2})\}\ (1<i<n/2) \tag{9}$$

The $\{S_1\}$ data on the horizontal axis are plotted against the values of the following series: 1, 2, 3, ..., (n/2) -1, n/2.

The data for $\{S_2\}$ are on the vertical axis according to the values: 1, 2, 3, ..., (n/2) -1, n/2.

According to Mandal et al. (2021), each series is then sorted independently in ascending order. The first half of the series (Xi) is plotted on the X axis and the second half of the series (Yi) is plotted on the Y axis. The presence of a trend is indicated by a 1:1 (45°) line in the scatterplot. The presence of a trend is indicated by a 1:1 (45°) line in the scatterplot. Coordinates on the 45° line indicate no trend, below it a negative trend, and above it an upward trend (Dabanli et al. 2016; Almazroui et al. 2019; Chowdari et al. 2023; Yaméogo 2025). A detailed interpretation of the ITAM is given in Figure 3 below, based on data from the present study at the Bobo-Dioulasso station.
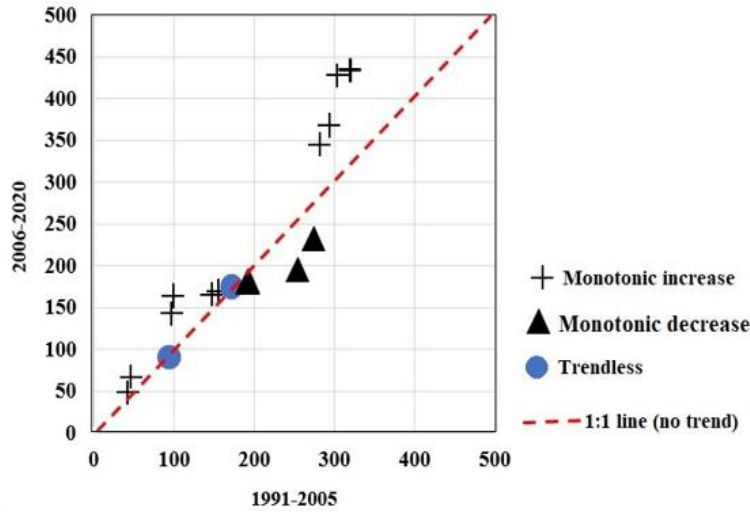
Fig. 3. Different interpretations of ITAM's results.

2.2.3. Slope (S) of ITAM

The slope trend S is calculated using the following expression (Şen 2017):

$$S = \frac{2 * (\bar{Y}_2 - \bar{Y}_1)}{n} \tag{10}$$

Where, $\bar{Y}_1$ and $\bar{Y}_2$ are the arithmetic means of the first series and the second half of the series of the dependent variable, and n is the number of data points.

2.2.3. The Percentage Bias Method (PBM)

The percentage bias method was used to estimate the percentage change in precipitation in the second half of the time series compared with the first half (Mandal et al. 2021):

$$PMB = 100 - \sum_{i=1}^{n} \frac{Y_i}{X_i} \times 100 \tag{11}$$

Where *PBM* is the percentage bias, n is the total extent of the sub-series separately, X_i and Y_i are the values of the observation data in the first and second sub-series, respectively. Positive and negative *PBM* values indicate increasing and decreasing trends, respectively, for the first sub-series.

2.2.4. Holt-Winters exponential smoothing model

The Holt-Winters method, which allows the seasonal model to adapt over time, is one of the best-known forecasting techniques (Lawton 1998). It involves estimating three smoothing parameters associated with level, trend, and seasonal variables (Atoyebi et al. 2023). Designed for trend and seasonal time series, the Holt-Winters method is a commonly used tool for forecasting trade data containing seasonality, changing trends, and seasonal correlation (Gelper et al. 2010). Several studies (Irwan et al. 2023) have also used this method to forecast hydro-climatological data series. The Holt-Winters approaches are modeled in one of two ways: additive or multiplicative (Koehler et al. 2001; Thomasson 2017; Natayu et al. 2022).

2.2.5. Holt-Winters seasonal additive model

The Holt-Winters additive method, which has a linear trend and constant seasonal variation (additive), has a prediction composed of the level (*Lt*), trend (*bt*), and seasonal variation (*st*) (Puah et al. 2016). The additive model incorporates seasonality but with the addition of a trend as follows (Pertiwi 2020; Wiguna et al. 2023):

- Level:

$$L_t = \alpha(Y_t - s_{t-c}) + (1 - \alpha)(L_{t-1} - b_{t-1}) \tag{12}$$

- Trend:

$$b_t = \beta(L_t - L_{t-1}) + (1 - \beta)b_{t-1} \tag{13}$$

- Seasonal:

$$s_t = \gamma(Y_t - L_t) + (1 - \gamma)s_{t-c} \tag{14}$$

The prediction for period F_{t+m} is:

$$F_{t+m} = L_t + b_{tm} + s_{t-s+m} \tag{15}$$

The smoothing parameters, α, β, and γ have values that vary between 0 and 1. In this study, the parameters are fixed at 0.2. This means that the prediction is flexible, i.e. strongly influenced by the most recent observations.

2.2.6. Multiplicative Holt-Winters method (MHW)

The multiplicative model is used if the data show variable seasonal fluctuations, and the different equations are as follows (Pleños 2022; Irwan et al. 2023; Wiguna et al. 2023):

- Level:

$$L_t = \alpha\frac{Y_t}{s_{t-s}} + (1 - \alpha)(L_{t-1} + b_{t-1}) \tag{16}$$

- Trend:

$$b_t = \beta(L_t - L_{t-1}) + (1 - \beta)b_{t-1} \tag{17}$$

- Seasonal:

$$S_t = \gamma\frac{Y_t}{L_t} + (1 - \gamma)S_{t-s} \tag{18}$$

The prediction period t is :

$$S_t = F_{t+m} = (L_t + b_t m)S_{t-s+m} \tag{19}$$

The smoothing parameters, α, β, and γ have values that vary between 0 and 1. In this study, the parameters are fixed at 0.2. This means that the prediction is flexible.

Where, Y_t – level in the 2nd period t; $L_{t-\alpha}$ – level in the 2nd period t-1; b_t – trend in the 2nd period t; b_{t-1} – trend in the 2nd period t-1; S_t – seasonality in the 2nd factors; Y_t – data in the 2nd period t; s – seasonal period; t – seasonal period; m – predictive time period.

2.2.7. Analysis of the Holt-Winters model performance

Goodness of fit is a critical criterion for assessing the accuracy of a predicted model relative to the true value (Atoyebi et al. 2023). Mean error (*ME*), *MSE* (mean squared error), *RMSE* (root mean squared error) and *MAPE* (mean absolute percentage error), mean absolute deviation (*MAD*), and mean squared deviation (*MSD*) have typically been used to examine model performance (Pinel 2020; Atoyebi et al. 2023). Other valuation parameters are also considered, such as the mean square error (*MSE*), the root mean square error (*RMSE*), and the mean absolute error (*MAE*). However, the use of *MAD* and *MSD* as indicators of prediction accuracy can be problematic in that they do not facilitate comparisons between different time series or time intervals, and the absolute measures *MAD* and *MSD* are affected by the size of the time series data (Atoyebi et al. 2023). The statistics *MAD* and *MSE*, provide no guidance on whether the model is good or not. This makes it impossible to use both measures (Gundalia, Dholakia 2012). Therefore, *MAPE* is used in studies as a valid indicator of model performance (Gundalia, Dholakia 2012; Puah et al. 2016). *MAPE* is also used in this study. *MAPE* consists of dividing the absolute error of each period by the true value of that period and calculating an average percentage of absolute errors (Wiguna et al. 2023). The mathematical formula used to calculate *MAPE* is as follows (Wiguna et al. 2023):

$$MAPE = \frac{1}{n}\sum_{t=1}^{n}\left|\frac{A_t - Y_t}{A_t}\right| \times 100\% \tag{20}$$

With, A_t – actual data; Y_t – forecasting data; n – number of periods. Prediction performance is interpreted using a prediction rating scale (Table 3). A summary of the methods used in the study is presented in Figure 4.

Table 3. Prediction model performance assessment scale (Gowri et al. 2022; Pinel 2020).

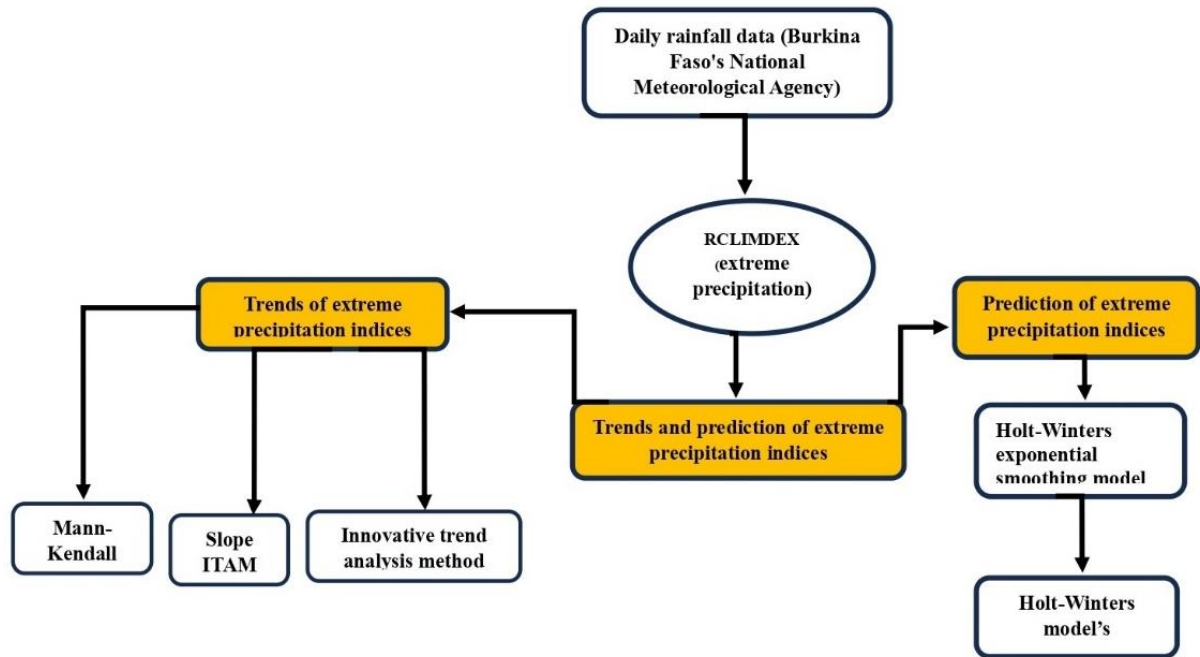| *MAPE*	Scale of interpretation	Significance
<10%	The ability to predict is very good	xxxxx
10-20%	Good ability of the model for prediction	xxxx
20-50%	The predictive ability of the model is feasible	xxx
>50%	Poor ability of the prediction model	x

Fig. 4. Data and methods used in the study.

3. Results

3.1. Descriptive statistics and test of extreme precipitation indices between 1991 and 2020

Table 4 shows that the extreme precipitation indices are highly variable for the Bobo-Dioulasso and Boromo stations and moderately variable for the Saria station over the period 1991-2020. The variability is particularly high for indices such as: r99ptot, r95ptot, cwd, R20mm, and Rx1day. Furthermore, the descriptive statistics show that the maxima and minima are relatively higher at the Bobo-Dioulasso station than at the other stations (Boromo and Koudougou). This difference could be explained by the climatic range of the stations. The Bobo-Dioulasso station is in the Sudanese zone (with precipitation of more than 900 mm per year). On the other hand, the other stations have low annual precipitation, which varies between 600 mm and 900 mm.

3.2. Trends in the indices of extreme precipitation between 1991 and 2020: an analysis using the Mann-Kendall test

The Mann-Kendall test shows that there was no trend in the extreme precipitation indices in the three cities of Burkina Faso over the period 1991-2020 (Table 5). The fact remains that a trend was observed for the frequency index (r99ptot) in the Bobo-Dioulasso station.

Table 4. Descriptive statistics for extreme precipitation indices from 1991 to 2020.

Station	Variable	Minimum	Maximum	Mean	Standard deviation	CV
Bobo-Dioulasso	Rx1day	38.1	114	68.9	18.1	26.27
	Rx5day	61.1	208	120.5	33.1	27.47
	sdii	10.2	18.5	14.3	2.1	14.69
	prcptot	675.1	1361.9	1024.7	176.6	17.23
	R10mm	25	45	34.4	5.5	15.99
	R20mm	11	26	18.2	3.8	20.88
	R95ptot	0	568.7	209.1	142.5	68.15
	R99ptot	0	263.7	57.1	74.5	130.47
	cdd	61	106	80.3	11	13.70
	cwd	3	12	5.3	1.9	35.85
	Variable	Minimum	Maximum	Mean	Standard deviation	CV
Boromo	Rx1day	44.2	134	75.7	26	34.35
	Rx5day	64.3	216.5	114.6	31.8	27.75
	SDII	10	17.5	14.3	1.8	12.59
	prcptot	643.1	1128.8	915.8	136.3	14.88
	R10mm	23	38	31.3	3.9	12.46
	R20mm	8	23	16	3.6	22.50
	R95ptot	44.2	434.4	199.9	110	55.03
	R99ptot	0	228	65	75	115.38
	cdd	50	117	82.4	15.4	18.69
	cwd	3	10	5	1.7	34
	Variable	Minimum	Maximum	Mean	Standard deviation	CV
Koudougou	Rx1day	50	127	73.1	19.2	26.27
	Rx5day	64	172	115.6	26.2	22.66
	SDII	10.8	17.7	14.3	1.5	10.49
	prcptot	624.8	1151.6	825.3	111.6	13.52
	R10mm	21	34	27.3	3.6	13.19
	R20mm	1	4	2	1	50
	R95ptot	54	307	174.2	75.7	43.46
	R99ptot	0	198	54.9	58.7	106.92
	cdd	63	133	92.8	18	19.40
	cwd	2	8	4.6	1.5	32.61

Table 5. Trend in extreme precipitation indices using the Mann-Kendall test.

	Index classification	Indices	Kendall's Tau	S	Var(S)	p-value	Trend	Trend direction
Bobo-Dioulasso station	Intensity indices Precipitation	rx1day	0.166	72.000	3140.667	0.205	no	-
		rx5day	0.124	54.000	3140.667	0.344	no	-
		sdii	0.136	59.000	3141.667	0.301	no	-
		prcptot	0.103	45.000	3141.667	0.432	no	-
	Frequency indices Precipitation	r10mm	0.082	35.000	3121.667	0.543	no	-
		r20mm	0.071	30.000	3104	0.603	no	-
		r95ptot	0.058	25.000	3137	0.668	no	-
		r99ptot	0.262	97.000	2648.333	**0.049**	**Yes**	**increase**
	Duration indices Precipitation	cdd	0.058	25.000	3133.667	0.668	no	-
		cwd	0.191	73.000	2881	0.180	no	-
Boromo station	Intensity indices Precipitation	rx1day	-0.018	-8.000	3140.667	0.901	no	-
		rx5day	0.085	37.000	3141.667	0.521	no	-
		sdii	0.154	67.000	3141.667	0.239	no	-
		prcptot	0.071	31.000	3141.667	0.592	no	-
	Frequency indices Precipitation	r10mm	0.093	39.000	3091.667	0.494	no	-
		r20mm	0.165	69.000	3093	0.221	no	-
		r95ptot	0.071	31.000	3141.667	0.592	no	-
		r99ptot	-0.140	-53.000	2732.333	0.320	no	-
	Duration indices Precipitation	cdd	-0.028	-12.000	3134	0.844	no	-
		cwd	0.003	1.000	2708.333	1.000	no	-
Saria station	Intensity indices Precipitation	rx1day	0	0.000	2558	1.000	no	-
		rx5day	-0.130	-49.000	2561	0.343	no	-
		sdii	0.212	80.000	2562	0.119	no	-
		prcptot	-0.074	-28.000	2562	0.594	no	-
	Frequency indices Precipitation	r10mm	-0.125	-46.000	2532.667	0.371	no	-
		r20mm	0.076	25.000	2332.333	0.619	no	-
		r95ptot	0.011	4.000	2562	0.953	no	-
		r99ptot	0.036	12.000	2293.333	0.818	no	-
	Duration indices Precipitation	cdd	-0.051	-19.000	2557	0.722	no	-
		cwd	-0.064	-22.000	2432.667	0.670	no	-

3.3. Trends in the indices of extreme precipitation between 1991 and 2020: an analysis using the innovative trend method

The innovative template trends method shows clear trends in the precipitation extremes indices according to the study stations.

3.3.1. Trends in the indices of extreme precipitation in the city of Bobo-Dioulasso

At this station, especially in the city of Bobo-Dioulasso, the precipitation intensity indices are increasing for prptot, rx5day, and sdii; rx1day decreased non-monotonically. For the extreme precipitation frequency indices, the trends are non-monotonic for r20mm, r10mm, and monotonic for r95ptot and r99ptot.

Conversely, the duration indices (cdd and cwd) are non-monotonic. Figure 5 summarises the trends of the extreme precipitation indices for the city of Bobo-Dioulasso over the period 1991-2020.

Figures 5b, 5c, and 5d, which group together precipitation intensity indices, show increases, in contrast to Figure 5a. The same applies to precipitation frequency indices. Figures 5f, 5g, and 5h, (but not 5e), are also increasing over the period 1991-2020. For the precipitation duration index, Figure 5i shows an increasing trend, while Figure 5j shows a non-monotonic increasing trend. The trends in extreme precipitation are increasing overall, and this situation could be explained by the climatic range in which the Bobo-Dioulasso station is located. The station is in the Sudanian zone, with annual precipitation in excess of 900 mm.
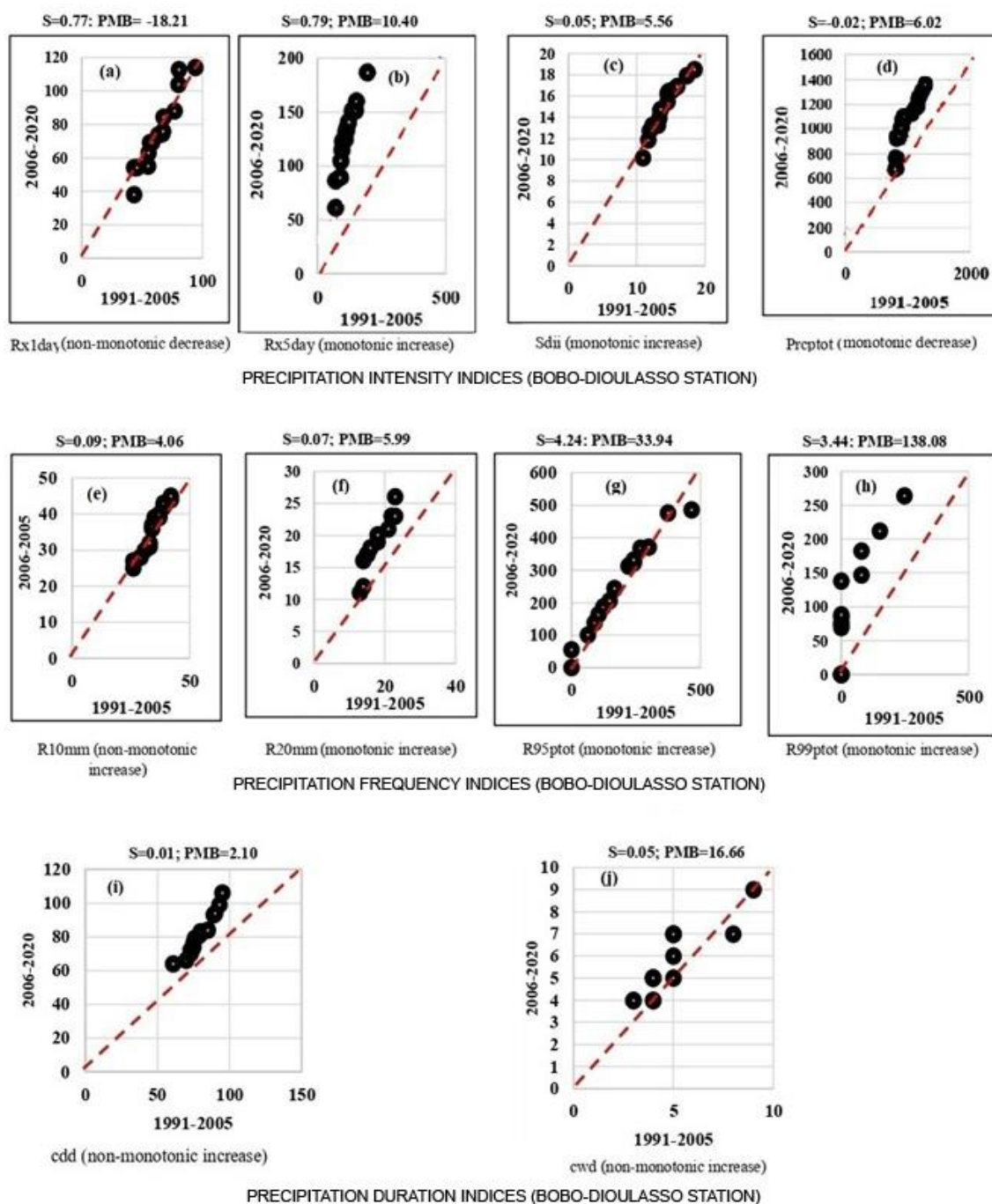

Fig. 5. Template trends of the extreme precipitation indices (station of Bobo-Dioulasso).

3.3.2. Trends in the indices of extreme precipitation in the city of Boromo

Figure 6 shows the graphical trends at the Boromo station in the town of Boromo. The precipitation intensity indices (Fig. 6b, 6c, 6d) increase monotonically. The precipitation frequency indices (Fig. 6e, 6f, 6h) are also increasing, with the exception of Figure 6g, which shows a non-monotonically increasing trend. In addition, the trends are non-monotonically decreasing in Figure 6i and non-monotonically increasing in Figure 6j.
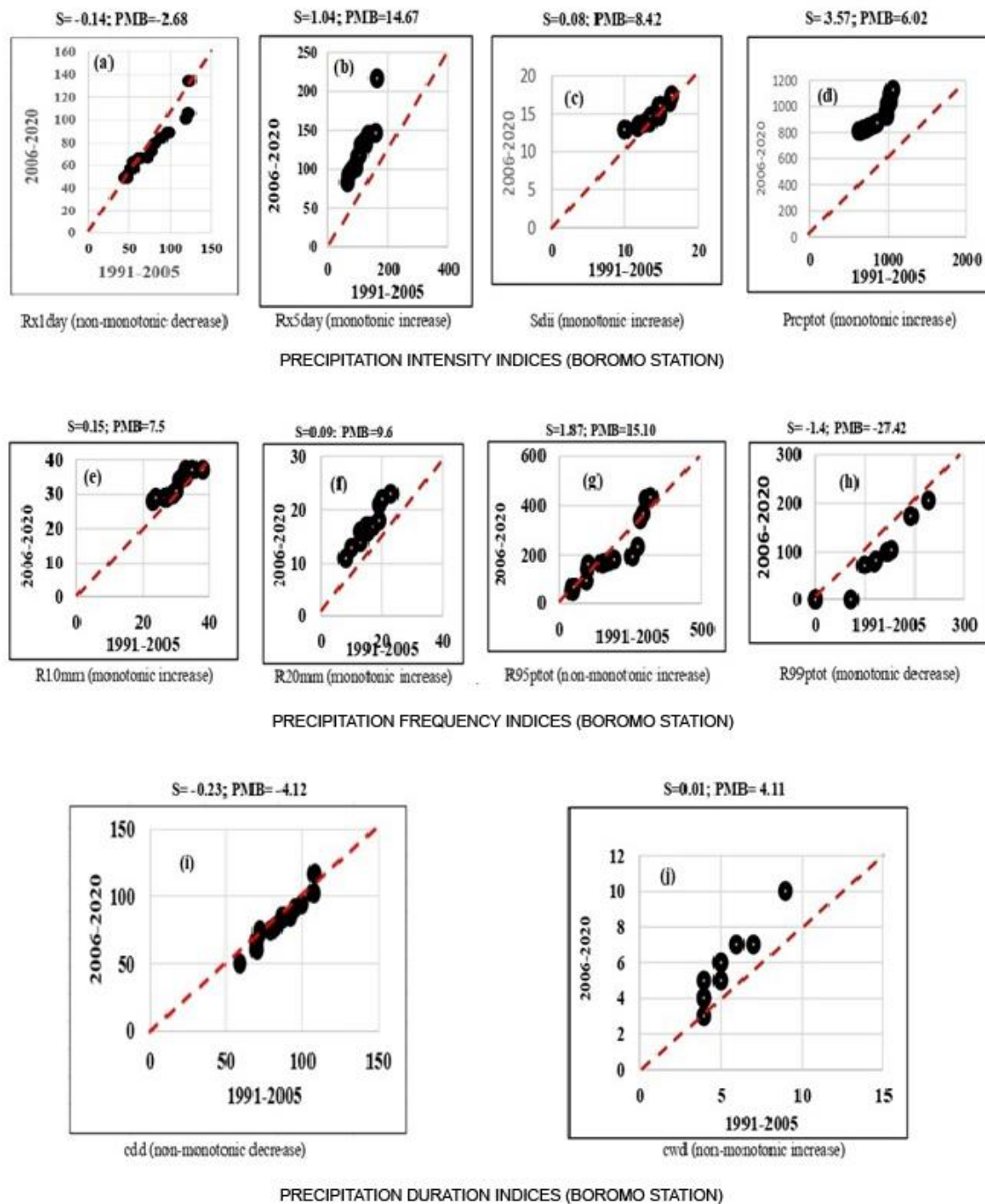

Fig. 6. Template trends of the extreme precipitation indices (Boromo station).

3.3.3. Trends in the indices of extreme precipitation in the city of City of Koudougou

The graphical trends of the extreme precipitation indices for the Saria station are more non-monotonic (Fig. 7). Extreme precipitation at the Saria station (city of Koudougou) shows unclear, even decreasing trends for precipitation duration indices, unlike the other two stations studied. This situation could be explained by the station's location in the Sudano-Sahelian region, where precipitation varies between 600 mm and 900 mm per year.
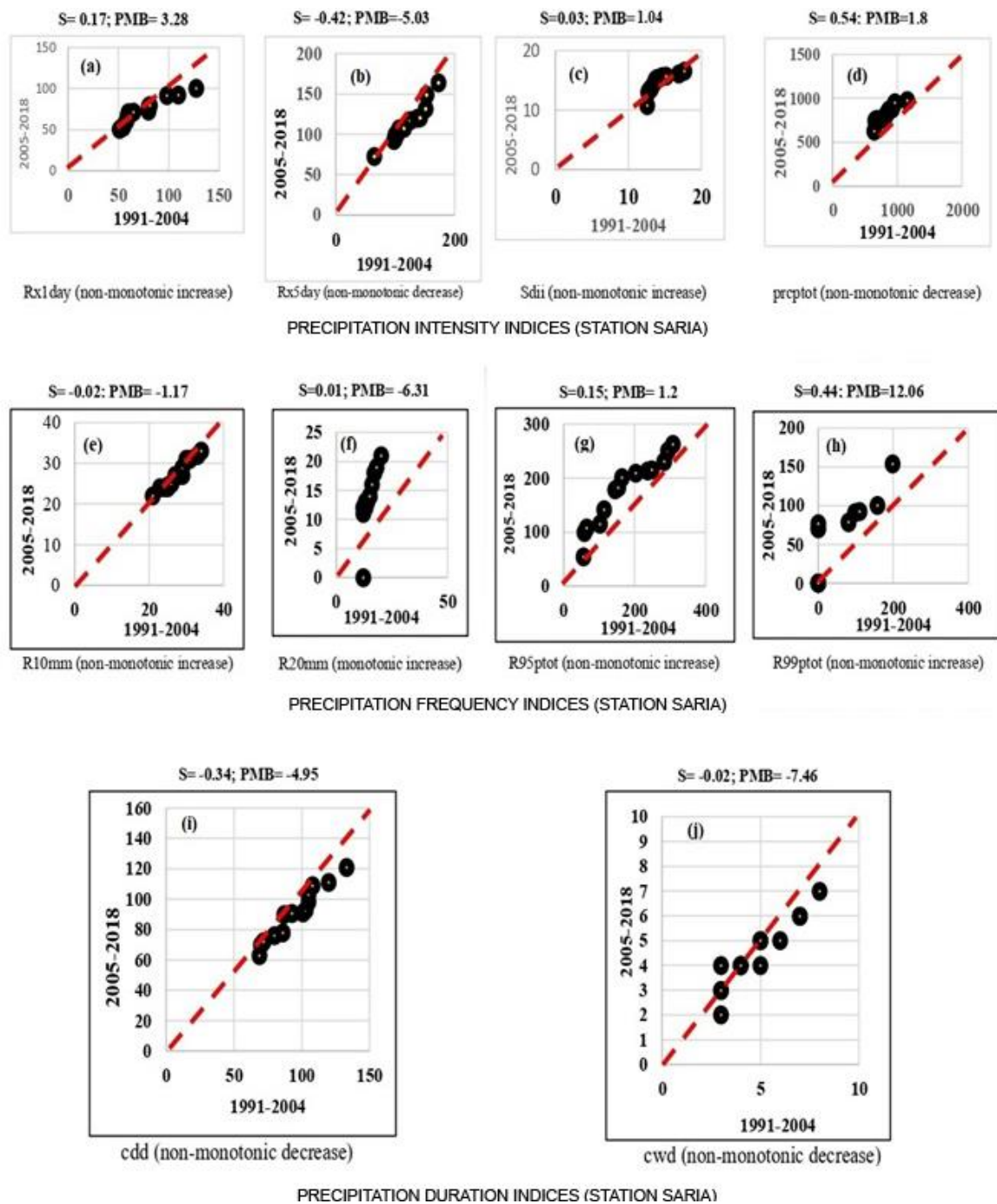

Fig. 7. Template trends of the extreme precipitation indices (station Saria).

3.4. Future projections of extreme precipitation indices for cities in Burkina Faso from 2020 to 2030

It is necessary to assess the performance of the Holt-Winters model to analyze the predicted precipitation indices for the three cities. Two models, additive and multiplicative, were used to assess the accuracy of the models proposed for each station. The prediction period is 10 years, specifically 2020-2030.

3.4.1. The case of the city of Bobo-Dioulasso (Bobo-Dioulasso station)

Table 6 shows that the additive Holt-Winters model is more accurate than the multiplicative Holt-Winters model based on the MAPE results. Nevertheless, the additive model does not fit R95ptot and R99ptot very well, with values of 86.05 and 73.7, respectively, indicating poor predictive ability of the model for these two indices. However, this model is more appropriate for the other extreme precipitation indices. This disparity leads to the use of the Holt-Winters additive model to analyze the future evolution of the extreme indices.

3.4.2. The case of the city of Boromo (Boromo station)

The performance of the additive and multiplicative models, according to MAPE, shows better accuracy for the additive model compared to the multiplicative model (Table 7). However, as at the Bobo-Dioulasso station, the additive model does not correctly adjust indices such as r95ptot and r99ptot.

3.4.3. The case of the city of Koudougou (Saria station)

As with the two stations above, the extreme precipitation index data applied to the additive and multiplicative models shows that the additive model provides a better fit for the extreme precipitation indices at the Saria station (Table 8).

Table 6. Results of the evaluation of the Holt-Winters additive and multiplicative models for the Bobo-Dioulasso station.

Index	Model parameters			Observation	DDL	SCE	MCE	RMCE	**MAPE**	MPE	MAE
	α	β	γ								
rx1day	0.2	0.2	0.2	30	14	8131.8	580.84	24.10	**24.27xxx**	-8.124	14.3
rx5day	0.2	0.2	0.2	30	14	41235	2945.36	54.3	**37xxx**	-13.686	37.8
sdii	0.2	0.2	0.2	30	14	172.5	12.32	3.5	**18xxxx**	-1.628	2.5
r10mm	0.2	0.2	0.2	30	14	1398.7	99.91	10	**20.5xxx**	0.409	7.3
r20mm	0.2	0.2	0.2	30	14	586.8	41.91	6.5	**30.6xxx**	-4.505	5.1
cdd	0.2	0.2	0.2	30	14	4441.5	317.25	17.8	**14.3xxxx**	-1.094	11.8
cwd	0.2	0.2	0.2	30	14	98.073	7	2.65	**37.8xxx**	-1.915	1.9
R95ptot	0.2	0.2	0.2	30	14	913811	65272.2	255.5	86.05x	-10.94	198
R99ptot	0.2	0.2	0.2	30	14	147205	10515	102.5	73.7x	21.68	70.8
prcptot	0.2	0.2	0.2	30	14	1074813	76772	277.07	20.9xxx	-0,590	205.3
Holt-Winters Seasonal Additive Model											
Index	Model parameters			Observation	DDL	SCE	MCE	RMCE	**MAPE**	MPE	MAE
	α	β	γ								
rx1day	0.2	0.2	0.2	30	14	8543.4	610.2	24.7	**26.2xxx**	-11.2	15.5
rx5day	0.2	0.2	0.2	30	14	45638.6	3259.9	57.1	**37.8xxx**	-20.2	36.4
sdii	0.2	0.2	0.2	30	14	171.1	12.2	3.5	**18xxxx**	-3.5	2.5
r10mm	0.2	0.2	0.2	30	14	1371.1	97.9	9.9	**21.7xxx**	-2.3	7.6
r20mm	0.2	0.2	0.2	30	14	574.2	41	6.4	**31xxx**	-8.8	5.1
cdd	0.2	0.2	0.2	30	14	5077.8	362.7	19	**16xxxx**	-2.9	13.1
cwd	0.2	0.2	0.2	30	14	113.4	8.1	2.8	**39.7xxx**	-13.5	2
r95ptot	0.2	0.2	0.2	30	14	1139410	81386.5	285.3	**100.6x**	-43.6	213
R99ptot	0.2	0.2	0.2	30	14	170915.7	12208.3	110.5	**83x**	15	71.9
prptot	0.2	0.2	0.2	30	14	1027791	73413.6	270.9	**20.9xxx**	-3	203.4
Multiplicative Holt-Winters method											

xxxxx: model is very good

xxxx: Good forecasting ability

xxx: Model's forecasting ability is feasible

x: Bad forecasting model ability

Table 7. Results of the evaluation of the Holt-Winters additive and multiplicative models for the Boromo station.

Index	Model parameters			Observations	DDL	SCE	MCE	RMCE	MAPE	MPE	MAE
	α	β	γ								
rx1day	0.2	0.2	0.2	30	14	31164.6	2226	47.2	**48.3ˣˣˣ**	-9.4	33.9
rx5day	0.2	0.2	0.2	30	14	48533	3466.6	59	**37.9ˣˣˣ**	-7.6	44.3
sdii	0.2	0.2	0.2	30	14	163	11.6	3.4	**18.4ˣˣˣˣ**	-1.0	2.7
r10mm	0.2	0.2	0.2	30	14	863.1	61.6	7.9	**19.1ˣˣˣˣ**	-2.5	6
r20mm	0.2	0.2	0.2	30	14	475	34	5.8	**25.8ˣˣˣ**	-3.2	4.3
cdd	0.2	0.2	0.2	30	14	8619	615.6	24.8	**21.7ˣˣˣ**	-3.8	16.6
cwd	0.2	0.2	0.2	30	14	118	8.4	2.9	**38.9ˣˣˣ**	-11.2	1.8
r95ptot	0.2	0.2	0.2	30	14	681573	48684	220.6	115.9ˣ	-55.2	162.4
r99ptot	0.2	0.2	0.2	30	14	301900	21564.3	146.8	**106.3ˣ**	73.7	111.7
prcptot	0.2	0.2	0.2	30	14	102563	73259.4	270.7	**23.4ˣˣˣ**	-2.2	212.2
Holt-Winters Seasonal Additive Model											
Index	Model parameters			Observations	DDL	SCE	MCE	RMCE	MAPE	MPE	MAE
	α	β	γ								
rx1day	0.2	0.2	0.2	30	14	33035	2359.6	48.5	53.7ˣ	-27.2	35.6
rx5day	0.2	0.2	0.2	30	14	60375	4312.5	65.7	**44.1ˣˣˣ**	-18.8	49.9
sdii	0.2	0.2	0.2	30	14	189.2	13.5	3.6	**20ˣˣˣˣ**	-3.8	2.9
r10mm	0.2	0.2	0.2	30	14	988	70.5	8.4	**20.2ˣˣˣ**	-5.3	6.3
r20mm	0.2	0.2	0.2	30	14	682.5	48.7	6.9	**31.2ˣˣˣ**	-10.3	5.1
cdd	0.2	0.2	0.2	30	14	8916	636.8	25.2	**22.3ˣˣˣ**	-5.8	16.9
cwd	0.2	0.2	0.2	30	14	135.4	9.6	3.1	**44.1ˣˣˣ**	-22.01	1.9
r95ptot	0.2	0.2	0.2	30	14	1815688	129691.9	360.1	211.8ˣ	-177.9	244.5
R99ptot	0.2	0.2	0.2	30	14	167615	11972.4	109.4	64.1ˣ	63.6	77.6
prcptot	0.2	0.2	0.2	30	14	1228361	87740	296.2	**25.2ˣˣˣ**	-6.6	226.3
Multiplicative Holt-Winters method											

xxxxx: model is very good

xxxx: Good forecasting ability

xxx: Model's forecasting ability is feasible

x: Bad forecasting model ability

Table 8. Results of the evaluation of the Holt-Winters additive and multiplicative models for the Boromo station.

Index	Model parameters			Observations	DDL	SCE	MCE	RMCE	**MAPE**	MPE	MAE
	α	β	γ								
rx1day	0.2	0.2	0.2	28	12	10161.9	846.8	29.1	**27.7xxx**	-1.8	21.4
rx5day	0.2	0.2	0.2	28	12	17430.9	1452.6	38.1	**21.7xxx**	-5.6	24.3
sdii	0.2	0.2	0.2	28	12	41.5	3.5	1.9	**8.9xxxxx**	2.2	1.3
r10mm	0.2	0.2	0.2	28	12	640.5	53.4	7.3	**20.4xxx**	-1.9	5.6
r20mm	0.2	0.2	0.2	28	12	33.3	2.8	1.7	53.8x	-17.3	1.1
cdd	0.2	0.2	0.2	28	12	15067	1255.6	35.4	**31xxx**	-2.5	26.5
cwd	0.2	0.2	0.2	28	12	135	11.3	3.4	68.2x	-28.5	2.5
r95ptot	0.2	0.2	0.2	28	12	147144	12262	110.7	**43.1xxx**	-5	75.6
r99ptot	0.2	0.2	0.2	28	12	67676.3	5639,7	75.1	71.9x	17.8	53.1
prcptot	0.2	0.2	0.2	28	12	553259	46101	214.7	**19.3xxxx**	-0.9	160.2
Holt-Winters Seasonal Additive Model											
Index	Model parameters			Observations	DDL	SCE	MCE	RMCE	**MAPE**	MPE	MAE
	α	β	γ								
rx1day	0.2	0.2	0.2	28	12	13309.3	1109.1	33.3	**31.3xxx**	-11.5	23.6
rx5day	0.2	0.2	0.2	28	12	18357	1529.7	39.1	**22.5xxx**	-9.7	24.7
sdii	0.2	0.2	0.2	28	12	38.2	3.2	1.8	**8.6xxxxx**	1.8	1.3
r10mm	0.2	0.2	0.2	28	12	672	56	7.5	**20.6xxx**	-4.3	5.6
r20mm	0.2	0.2	0.2	28	12	65.6	5.5	2.3	77.7x	-52.1	1.5
cdd	0.2	0.2	0.2	28	12	14366.2	1197.2	34.6	**30.8xxx**	-7.2	26
cwd	0.2	0.2	0.2	28	12	157.4	13.1	3.6	74x	-49.6	2.5
R95ptot	0.2	0.2	0.2	28	12	315065	26255.4	162	62.2x	-38.4	110.7
R99ptot	0.2	0.2	0.2	28	12	75320.3	6276.7	79.2	83x	38	59.4
prcptot	0.2	0.2	0.2	28	12	521007	43417	208.4	**19xxxxx**	-3.8	155.5
Multiplicative Holt-Winters method											

xxxxx: model is very good

xxxx: Good forecasting ability

xxx: Model's forecasting ability is feasible

X: Bad forecasting model ability

3.5. Projection trajectories between 2020 and 2030 for extreme precipitation indices

Because the additive model is a better fit to the extreme precipitation index data from the study stations, this model is adopted for future predictions for the period 2020-2030. In addition, the fit of the model varies between the study stations. Therefore, the analyses are based on the study stations.

3.5.1. The case of the city of Bobo-Dioulasso (Bobo-Dioulasso station)

The results of the predictions for the 2030 period show that the precipitation intensity indices (rx1day, r5day, sdii, and prcptot) and the precipitation frequency indices (r10mm, r20mm, r95ptot, r99ptot) will increase between 2020 and 2030. The situation is different for the precipitation duration indices, with CDD steadily increasing until 2030 and CWD decreasing over the same period (Fig. 8). In the figure, blue indicates observed precipitation extremes, and red lines indicate the Holt-Winters prediction of precipitation extremes. The dotted green line indicates the trend. The figure shows that the indices rx5day and cwd display downward trends until 2030. On the other hand, the other indices (rx1day, sdii, prcpot, r10mm, r20mm, r95pot, r99pot) show increasing trends until 2030. Given this situation, flooding and water-borne diseases are likely to be a problem in the city in the coming years.

3.5.2. The case of the city of Boromo (Boromo station*)*

At this station, precipitation intensity and duration indices are increasing (Fig. 9). However, the precipitation frequency indices show different trends. R10mm and r99ptot decrease, while r20mm and r95ptot increase from 2020 to 2030.

3.5.3. The case of the city of Koudougou (Saria station)

The precipitation intensity indices show different trends. In fact, rx1day and rx5day are decreasing, while sdii and prcptot increase continuously from 2020 to 2030. The same is true for the precipitation frequency indices, which show a decreasing trend for r10mm, r95ptot, and r99ptot. The only frequency index that increases is r20mm. In addition, the precipitation duration indices increase from 2020 to 2030. The city of Koudougou should suffer less from climatic disasters than the other two cities, in the sense that intensity and frequency are low over the period 2020-2030. However, the increase in precipitation duration will be detrimental to farmers on the outskirts of the city and urban market gardeners. Figure 10 shows the changes in extreme precipitation indices from 2020 to 2030. The figure shows that two forecast trends are also noticeable at the Saria station. In contrast to the other stations, the forecast trends are more negative than positive. The downward trends are represented by Figure 10 (rx1day), (rx5day). Conversely, Figure 10 (sdii), (prcptot), (r20mm), and (cdd) shows upward trends. Thus, the city of Koudougou may be less affected by extreme precipitation than the other two cities of Bobo-Dioulasso and Boromo.
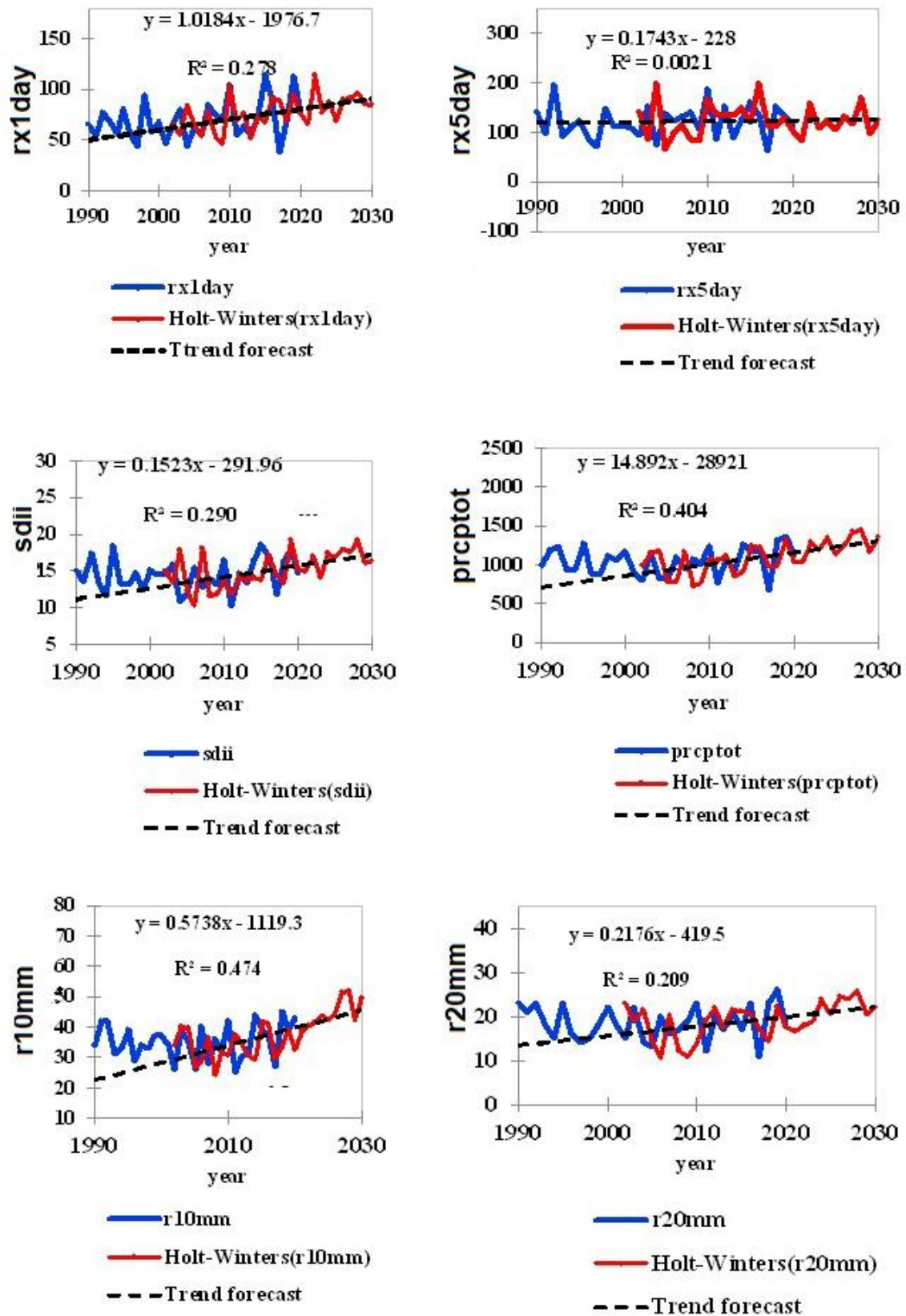
Fig. 8. Predictions of the changes in the indices of extreme precipitation for the station of Bobo-Dioulasso.
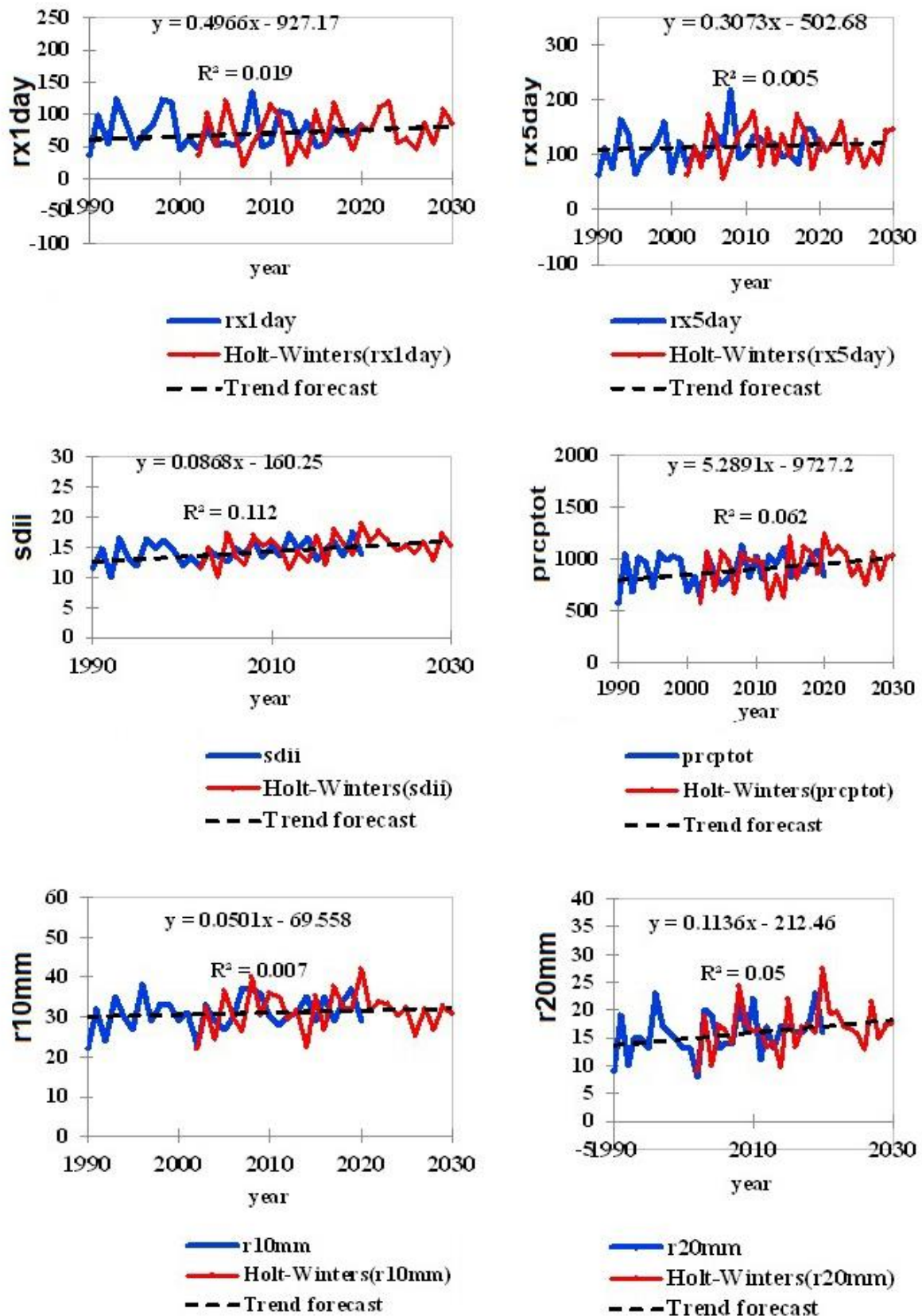
Fig. 9. Predictions of the changes in the indices of extreme precipitation for the station of Boromo.
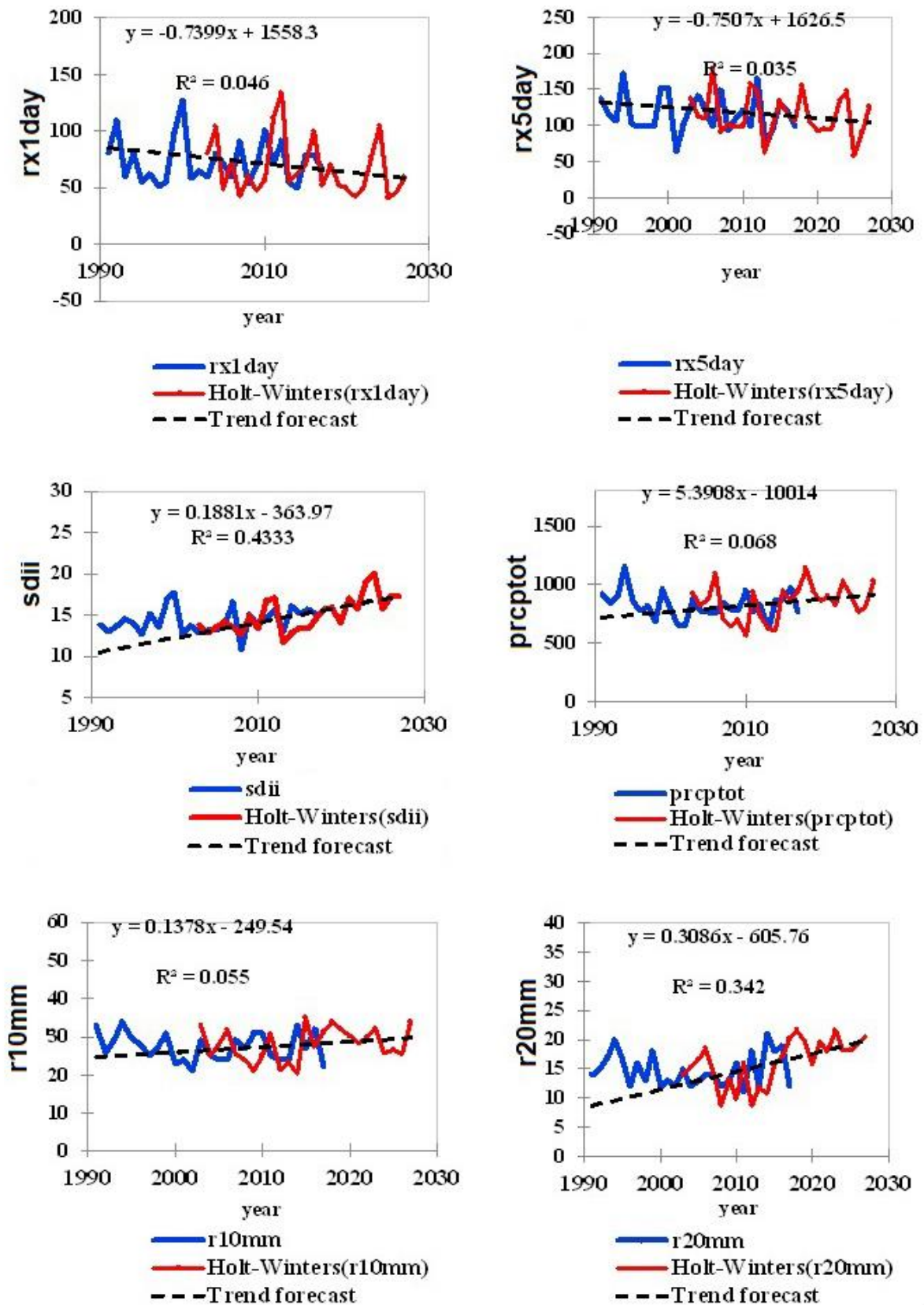
Fig. 10. Predictions of the changes in the indices of extreme precipitation for the station of Saria.

4. Discussion

4.1. Analysis of inter-annual variability and trends in extreme precipitation indices in West Africa

Time series are records of processes that change over time (Ihaka 2005). This study has shown strong variability in extreme precipitation indices at the three study stations. In addition, the extreme precipitation indices showed a continuous increase from 1991 to 2020. The results confirm the work of other authors in Burkina Faso and West Africa (Bigi et al. 2018). Indeed, extreme precipitation indices such as rx1day, rx5day, prcptot, and sdii increased and r95ptot decreased from 1991 to 2021 in the Boucle du Mouhoun region of Burkina Faso (Rouamba et al. 2023). Yanogo and Yaméogo (2023) also note that indices such as prcptot and r95ptot are increasing for the Ouahigouya station in Burkina Faso. These results are confirmed by the study of Tazen et al. (2019) in Burkina Faso, which showed an upward trend in indices such as Rx1day, Rx5day, and r99ptot from 1961 to 2015. This trend has also been observed in other West African countries by various authors. In Niamey, Niger, the same indices (rx1day, rx5day, prcptot) also increased between 1990 and 2020 (Bassirou et al. 2023). Bigi et al. (2018) add that a similar trend was observed in Niamey city (Niger) between 1980 and 2009. This confirms the studies by Konate et al. (2023) in Côte d'Ivoire during 1961-2015. Indeed, the authors note that indices such as prcptot, sdii, rx1day, rx5day, r20mm, r95ptot, and r99ptot increased in Ivorian cities (Gagnoa, Daloa, Yamoussoukro), while cdd and cwd decreased between 1961 and 2015. In other cities (Korhogo, Odienné, Bondoukou, Man, Abidjan, Adiaké, San-Pedro, Tabou, Sassandra), indices such as prcptot, sdii, CDD, CWD, R10mm, and R20mm show significantly negative trends (Konate et al. 2023). The exception is San-Pedro, which shows significantly positive trends for the prcptot, sdii, CDD, and R10mm indices. This situation shows that when the zones are located in the Ivory Coast's Sudanese-type climate, the trends of the indices are negative. On the other hand, when the zones are located in the Baulean-type climate zones, the extreme precipitation indices tend to show positive trends overall. Furthermore, in the Attean climate, the precipitation indices are positive overall. It is therefore clear that the trends vary according to the climatic zone, a situation that is also revealed by the results of the zones studied using the innovative method.

4.2. Analysis of the predictions of the extreme precipitation index

Forecasting precipitation is important for two reasons: it is a major scientific challenge, but it is also crucial for planning and developing agricultural strategies (Graham, Mishra 2017). In the study cities, precipitation intensity and frequency indices are expected to increase between 2020 and 2030 in the large city of Bobo-Dioulasso, the medium-sized city of Koudougou, and the small city of Boromo. However, the city of Koudougou should be less affected than the other two cities, as many extreme indices such as cdd, r95ptot, r99ptot, r10mm, rx1day and rx5day will decrease continuously until 2030. These results are consistent with those for Africa (Abiodun et al. 2017). Indeed, the authors note that coastal cities will experience an increase in extreme precipitation indices, with cities such as Maputo, Logos, and Port Said expected to experience an increase in the intensity and frequency of extreme precipitation between 2081 and 2100. Other authors, such as Biasutti (2013) and Trepekli et al. (2019), note that precipitation is

expected to be concentrated in more intense extreme precipitation events, interspersed with long periods of low precipitation over the West African Sahel. Another study conducted in Africa by Habiyakare et al. (2024) confirms the findings of the previous authors. In fact, according to these authors, West Africa, East Africa, and the eastern part of South Africa show an increasing trend in extreme precipitation, and changes in extreme precipitation indices show a general increase in the occurrence and frequency of extreme precipitation indices in all scenarios by the end of the 21st century.

4.3. The sources of uncertainty and limitations of the methods

Precipitation in Burkina Faso tends to be erratic from month to month and season to season. This makes it difficult to make accurate forecasts. The Holt-Winters exponential smoothing method is therefore used in this study. This method has clear advantages because it accounts for trends and seasonality (Pongdatu, Putra 2018), which corresponds to the characteristics of precipitation in the tropics. This situation has led other authors (Pertiwi 2020) to use this method in the tropics. However, this method has shortcomings that need to be considered. The method is deterministic because for each point in the future, the forecast provides a single value that approximates the future outcome. It does not allow other possibilities to be considered. In addition, exponential smoothing forecasting techniques only consider historical data, which means that they ignore any information that may be generated at the same time (Pardoux, Goldfarb 2013). Pinel (2020) adds that the Holt-Winters method has three major shortcomings: first, there is no guarantee that the method is optimal for a given data series; exponential smoothing methods are sometimes far from optimal. In addition, forecasts are more accurate in the short term (a few years). On the other hand, they cannot provide forecast intervals, i.e. an interval containing the forecast with a given probability. This is because a probabilistic framework has not yet been defined. Thus, the results of the forecasting study are limited. Indeed, if the period considered is intermediate (2020-2030), the forecasts of the Holt-Winters method become less accurate as the time considered is extended. In this study, therefore, the forecast for the first five years (2020-2025) is more accurate than that for the remaining five years (2025-2030). In addition, the data analysis is done with software that only allows models of deterministic precision as mean square error, and the choice of parametric models is limited to 0.2 α, β, and γ. These constraints do not allow for any flexibility in the accuracy of the forecasts. Nevertheless, our results provide decision-makers with an indication of the evolution of extreme precipitation indices over the period 2020-2030, with greater accuracy between 2020 and 2025, given the short-term option of the forecasting method.

5. Conclusions

The study analyzed the trends and projected trajectories of extreme precipitation indices in the cities of Burkina Faso. The precipitation intensity and frequency indices are variable, with an upward trend for the cities of Bobo-Dioulasso, Boromo, and Koudougou. Template trends also show a steady increase in precipitation intensity and frequency indices for the cities of Bobo-Dioulasso and Boromo. For the city of Koudougou, a non-monotonic increasing trend is observed for the precipitation intensity and frequency indices. The rain duration indices show a non-monotonic decreasing trend. The Holt-Winters method can

be used to make short-term predictions. This method was used to predict extreme precipitation indices between 2020 and 2030, which are increasing for the intensity and frequency indices in the cities of Bobo-Dioulasso and Boromo. However, the indices have relatively high variability, accompanied by an upward trend over the period 2020-2030. Under these conditions, the authorities in the affected towns should give absolute priority to widening the gutters to allow rainwater to drain away. In addition, the town of Boromo is in a special situation compared to the others, since its population has increased in response to internal migration caused by terrorism in the country. The migrants have settled in flood-prone areas, and the local authorities should encourage them to move away from easily flooded areas.

References

Abiodun B.J, Adegoke J., Abatan A.A., Ibe C.A., Egbebiyi T.S., Engelbrecht F., Pinto I., 2017, Potential impacts of climate change on extreme precipitation over four African coastal cities, Climatic Change, 143, 399-413, DOI: 10.1007/s10584-017-2001-5.

Aditya F., Gusmayanti E., Sudrajat J., 2021, Rainfall trend analysis using Mann-Kendall and Sen's slope estimator test in West Kalimantan, IOP Conference Series: Earth and Environmental Science, 893 (1), DOI: 10.1088/1755-1315/893/1/012006.

Almazroui M., Şen Z., Mohorji A.M., Islam M.N., 2019, Impacts of climate change on water engineering structures in arid regions: case studies in Turkey and Saudi Arabia, Earth Systems and Environment, 3, 43-57, DOI: 10.1007/s41748-018-0082-6.

Atoyebi S.B., Olayiwola M.F., Oladapo J.O., Oladapo D.I., 2023, Forecasting Currency in Circulation in Nigeria Using Holt-Winters Exponential Smoothing Method, South Asian Journal of Social Studies and Economics, 20 (1), 25-41, DOI: 10.9734/sajsse/2023/v20i1689.

Barry A.A., Caesar J., Klein Tank A.M.G., Aguilar E., McSweeney C., Cyrille A.M., Nikiema M.P., Narcisse K.B., Sima F., Stafford G., Touray L.M., Ayilari-Naa J.A., Mendes C.L., Tounkara M., Gar-Glahn E.V.S., Coulibaly M.S., Dieh M.F., Mouhaimouni M., Oyegade J.A., Sambou E., Laogbessi E.T., 2018, West Africa climate extremes and climate change indices, International Journal of Climatology, 38 (S1), e921-e938, DOI: 10.1002/joc.5420.

Bassirou H., Masamaéya D.T.G., Sanda I.S., Cheo A.E., Sougue M., Pouye I., 2023, Extreme rainfall and streamflow in Niamey City: Trends and relationship between higher streamflow and rainfall, International Journal of Water Resources Engineering, 9 (1), 21-32, DOI: 10.37628/jwre.v9i1.802.

Béwentaoré S., Barro D., 2022, Space-time trend detection and dependence modeling in extreme event approaches by functional peaks-over-thresholds: Application to precipitation in Burkina Faso, International Journal of Mathematics and Mathematical Sciences, 1, DOI: 10.1155/2022/2608270.

Bhagat S.K., Ramaswamy K., 2023, Precipitation variations in the central Vietnam to forecast using Holt-Winters Seasonal Additive Forecasting method for 1990 to 2019 trend, IOP Conference Series: Earth and Environmental Science, 1216 (1), DOI: 10.1088/1755-1315/1216/1/012019.

Biasutti M., 2013, Forced Sahel rainfall trends in the CMIP5 archive, Journal of Geophysical Research: Atmospheres, 118 (4), 1613-1623, DOI: 10.1002/jgrd.50206.

Bigi V., Pezzoli A., Rosso M., 2018, Past and future precipitation trend analysis for the City of Niamey (Niger): An overview, Climate, 6 (3), DOI: 10.3390/cli6030073.

Chowdari K.K., Deb Barma S., Bhat N., Girisha R., Gouda K.C., Mahesha A., 2023, Trends of seasonal and annual rainfall of semi-arid districts of Karnataka, India: application of innovative trend analysis approach, Theoretical and Applied Climatology, 152 (1), 241-264, DOI: 10.1007/s00704-023-04400-9.

Dabanli İ., Şen Z., Yeleğen M.O., Şişman E., Selek B., Güçlü Y.S., 2016, Trend assessment by the innovative-Şen method, Water Resources Management, 30 (14), 5193-5203, DOI: 10.1007/s11269-016-1478-4.

Diémé L.P.M., Bouvier C., Bodian A., Sidibé A., 2025, Detection of flooding by overflows of the drainage network: Application to the urban area of Dakar (Senegal), Natural Hazards and Earth System Sciences, 25, 1095-1112, DOI: 10.5194/egusphere-2023-2458.

Doan Q.-V., Kobayashi S., Kusaka H., Chen F., He C., Niyogi D., 2023, Tracking urban footprint on extreme precipitation in an African megacity, Journal of Applied Meteorology and Climatology, 62 (2), 209-226, DOI: 10.1175/JAMC-D-22-0048.1.

Ezeh A., Kissling F., Singer P., 2020, Why sub-Saharan Africa might exceed its projected population size by 2100, The Lancet, 396 (10258), 1131-1133, DOI: 10.1016/S0140-6736(20)31522-1.

Gbode I.E., Adeyeri O.E., Menang K.P., Intsiful J.D., Ajayi V.O., Omotosho J.A., Akinsanola A.A., 2019, Observed changes in climate extremes in Nigeria, Meteorological Applications, 26 (4), 642-654, DOI: 10.1002/met.1791.

Gelper S., Fried R., Croux C., 2010, Robust forecasting with exponential and Holt–Winters smoothing, Journal of forecasting, 29 (3), 285-300, DOI: 10.1002/for.1125.

Gimeno L., Sorí R., Vazquez M., Stojanovic M., Algarra I., Eiras-Barca J., Gimeno-Sotelo L., Nieto R., 2022, Extreme precipitation events, Wiley Interdisciplinary Reviews: Water, 9 (6), DOI: 10.1002/wat2.1611.

Giugni M., Simonis I., Bucchignani E., Capuano P., De Paola F., Engelbrecht F., Mercogliano P., Topa M.E., 2015, The impacts of climate change on African cities, [in:] Urban Vulnerability and Climate Change in Africa: A Multidisciplinary Approach, Springer, 37-75. DOI: 10.1007/978-3-319-03982-4_2.

Gowri L., Manjula K.R., Sasireka K., Deepa D., 2022, Assessment of statistical models for rainfall forecasting using machine learning technique, Journal of Soft Computing in Civil Engineering, 6(2), 51-67, DOI: 10.22115/SCCE.2022.304260.1363.

Graham A., Mishra E.P., 2017, Time series analysis model to forecast rainfall for Allahabad region, Journal of Pharmacognosy and Phytochemistry, 6 (5), 1418-1421.

Gundalia M.J., Dholakia M.B., 2012, Prediction of maximum/minimum temperatures using Holt Winters method with Excel spreadsheet for Junagadh region, International Journal of Engineering Research and Technology, 1 (6), DOI: 10.17577/IJERTV1IS6301.

Güçlü Y.S., 2020, Improved visualization for trend analysis by comparing with classical Mann-Kendall test and ITA, Journal of Hydrology, 584, DOI: 10.1016/j.jhydrol.2020.124674.

Habiyakare F., Jiang T., Yahaya I., Ndabagenga D., Kagabo J., Su B., 2024, Spatial variation and trend of extreme precipitation in Africa during 1981-2019 and its projected changes at the end of 21st century, Journal of Geoscience and Environment Protection, 12 (3), 192-221, DOI: 10.4236/gep.2024.123012.

Herslund L., Lund D.H., Jørgensen G., Mguni P., Kombe W.J., Yeshitela K., 2015, Towards climate change resilient cities in Africa–Initiating adaptation in Dar es Salaam and Addis Ababa, [in] Urban Vulnerability and Climate Change in Africa: A Multidisciplinary Approach, Springer, 319-348, DOI: 10.1007/978-3-319-03982-4_10.

Ihaka R., 2005, Time Series Analysis, Lecture Notes for 475726, Statistics Department, University of Auckland.

INSD, 2011, Le Burkina en chiffres, 8, Institut National de la Statistique et de la Démographie.

IPCC, 2021, Summary for Policymakers, [in:] Climate Change 2021: The Physical Science Basis. Contribution of Working Group I to the Sixth Assessment Report of the Intergovernmental Panel on Climate Change, IPCC.

IPCC, 2023, Climate Change 2023: Synthesis Report. Contribution of Working Groups I, II and III to the Sixth Assessment Report of the Intergovernmental Panel on Climate Change, Core Writing Team, H. Lee and J. Romero (eds.), IPCC, Geneva, Switzerland, DOI: 10.59327/IPCC/AR6-9789291691647.

Irwan I., Abdy M., Karwingsi E., Ahmar A.S., 2023, Rainfall forecasting in Makassar City using triple exponential smoothing method, ARRUS Journal of Social Sciences and Humanities, 3 (1), 52-58, DOI: 10.35877/soshum1707.

Karl T.R., Nicholls N., Anver G., 1999, CLIVAR/GCOS/WMO Workshop on indices and indicators for climate extremes workshop summary, [in:] Weather and Climate Extremes: Changes, Variations and a Perspective from the Insurance Industry, T.R. Karl, N. Nicholls. Ghazi A. (eds.), Springer, Dordrecht, 3-7, DOI: 10.1007/978-94-015-9265-9_2.

Kessabi R., Hanchane M., Ait Brahim Y., El Khazzan B., Addou R., Belmahi M., 2024, Characterization of annual and seasonal rainfall trend using innovative trend analysis (ITA) and classical methods: the case of Wadi Sebou basin (WSB) Morocco, Euro-Mediterranean Journal for Environmental Integration, 10, 555-573, DOI: 10.1007/s41207-024-00507-1.

Koala S., Nakoulma G., Dipama J.-M., 2023, Évolution des précipitations et de la température à l'Horizon 2050 avec les modèles climatiques CMIP5 dans le bassin versant du Nakambé (Burkina Faso), International Journal of Progressive Sciences and Technologies, 37 (2), 110-124, DOI: 10.52155/ijpsat.v37.2.5133.

Koehler A.B., Snyder R.D., Ord J.K., 2001, Forecasting models and prediction intervals for the multiplicative Holt–Winters method, International Journal of Forecasting, 17 (2), 269-286, DOI: 10.1016/S0169-2070(01)00081-4.

Konate D., Didi S.R., Dje K.B, Diedhiou A., Kouassi K.L., Kamagate B., Paturel J.-E., Coulibaly H.S.J.-P., Kouadio C.A.K., Coulibaly T.J.H., 2023, Observed changes in rainfall and characteristics of extreme events in Côte d'Ivoire (West Africa), Hydrology, 10(5), 104, DOI: 10.3390/hydrology10050104.

Kougbeagbede H., 2024, Detection of annual rainfall trends using innovative trend analysis method in Benin, International Journal of Global Warming, 32 (1), 54-64, DOI: 10.1504/IJGW.2024.135361.

Lawton R., 1998, How should additive Holt–Winters estimates be corrected?, International Journal of Forecasting, 14 (3), 393-403, DOI: 10.1016/S0169-2070(98)00040-5.

Lourdes F.M., Kim Y.K., Choi M., Kim J.-C., Do X.K., Nguyen T.H., Jung K., 2021, Detailed trend analysis of extreme climate indices in the Upper Geum River Basin, Water, 13 (22), DOI: 10.3390/w13223171.

Mallick J., Talukdar S., Alsubih M., Salam R., Ahmed M., Kahla N.B., Shamimuzzaman M., 2021, Analysing the trend of rainfall in Asir region of Saudi Arabia using the family of Mann-Kendall tests, innovative trend analysis, and detrended fluctuation analysis, Theoretical and Applied Climatology, 143, 823-841, DOI: 10.1007/s00704-020-03448-1.

Mandal T., Sarkar A., Das J., Rahman A.T.M.S., Chouhan P., 2021, Comparison of classical Mann-Kendal test and graphical innovative trend analysis for analyzing rainfall changes in India, [in:] India: Climate Change Impacts, Mitigation and Adaptation in Developing Countries, Cham: Springer International Publishing, 155-183, DOI: 10.1007/978-3-030-67865-4_7.

Marak J.D.K., Sarma A.K., Bhattacharjya R.K., 2020, Innovative trend analysis of spatial and temporal rainfall variations in Umiam and Umtru watersheds in Meghalaya, India, Theoretical and Applied Climatology, 142, 1397-1412, DOI: 10.1007/s00704-020-03383-1.

Mohorji A.M., Şen Z., Almazroui M., 2017, Trend analyses revision and global monthly temperature innovative multi-duration analysis, Earth Systems and Environment, 1, DOI: 10.1007/s41748-017-0014-x.

Muthiah M., Sivarajan S., Madasamy N., Natarajan A., Ayyavoo R., 2024, Analyzing Rainfall trends using statistical methods across Vaippar Basin, Tamil Nadu, India: A comprehensive study, Sustainability, 16 (5), DOI: 10.3390/su16051957.

Natayu A., Clarke Q.J.H., Fikri M., 2022, Benchmark of Holt–Winters and SARIMA methods in predicting Jakarta climate, preprints.

Nurhamidah N., Nusyirwan N., Faisol A., 2020, Forecasting seasonal time series data using the holt-winters exponential smoothing method of additive models, Jurnal Matematika Integratif, 16 (2), 151-157, DOI: 10.24198/jmi.v16.n2.29293.151-157.

OECD, 2022, Africa's Urbanisation Dynamics 2022. The Economic Power of Africa's Cities, West African Studies, OECD/UN ECA/AfDB, OECD Publishing, Paris, DOI: 10.1787/3834ed5b-en.

Oufrigh O., Elouissi A., Benzater B., 2023, Trend assessment by the Mann-Kendall test and the Innovative Trend Analysis method (North-West Algeria), GeoScience Engineering, 69 (2), 186-233, DOI: 10.35180/gse-2023-0099.

Pala Z., Şevgin F., 2024, Statistical modeling for long-term meteorological forecasting: a case study in Van Lake Basin, Natural Hazards, 120, 14101-14116, DOI: 10.1007/s11069-024-06747-2.

Pardoux C., Goldfarb B., 2013, Prévision à court terme: méthodes de lissage exponentiel, Université de Paris Douphien, 52 pp.

Pastagia J., Mehta D., 2022, Application of innovative trend analysis on rainfall time series over Rajsamand district of Rajasthan state, Water Supply, 22 (9), 7189-7196, DOI: 10.2166/ws.2022.276.

Patel S., Mehta D., 2023, Statistical analysis of climate change over Hanumangarh district, Journal of Water and Climate Change, 14 (6), 2029-2041, DOI: 10.2166/wcc.2023.227.

Pertiwi D.D., 2020, Applied exponential smoothing Holt-Winters method for rainfall forecast in Mataram City, Journal of Intelligent Computing and Health Informatics, 1 (2), 46-49, DOI: 10.26714/jichi.v1i2.6330.

Pinel S., 2020, Ajustement de courbes et séries chronologiques, IUT STID, UE21 M2102, 37 pp.

Pleños M., 2022, Time series forecasting using holt-winters exponential smoothing: Application to abaca fiber data, Zeszyty Naukowe SGGW w Warszawie – Problemy Rolnictwa Światowego, 22 (2), 17-29, DOI: 10.22630/PRS.2022.22.2.6.

Pongdatu G.A.N., Putra Y.H., 2018, Seasonal time series forecasting using SARIMA and Holt Winter's exponential smoothing, IOP Conference Series: Materials Science and Engineering, 407 (1), DOI: 10.1088/1757-899X/407/1/012153.

Puah Y.J., Huang Y.F., Chua K.C., Lee T.S., 2016, River catchment rainfall series analysis using additive Holt–Winters method, Journal of Earth System Science, 125 (2), 269-283, DOI: 10.1007/s12040-016-0661-6.

Rouamba S., Yaméogo J., Sanou K., Zongo R., Yanogo I.P., 2023, Trends and variability of extreme climate indices in the Boucle du Mouhoun (Burkina Faso), GEOREVIEW: Scientific Annals of Stefan cel Mare University of Suceava: Geography Series, 33 (1), 70-84, DOI: 10.4316/GEOREVIEW.2023.01.07.

Sanusi W., Abdy M., 2021, Innovative trend analysis of annual maximum precipitation in Gowa regency, Journal of Physics: Conference Series, 1899 (1), DOI: 10.1088/1742-6596/1899/1/012092.

Şen Z., 2017, Innovative trend significance test and applications, Theoretical and Applied Climatology, 127, 939-947, DOI: 10.1007/s00704-015-1681-x.

Şen Z., Şişman E., Dabanli I., 2019, Innovative polygon trend analysis (IPTA) and applications, Journal of Hydrology, 575, 202-210, DOI: 10.1016/j.jhydrol.2019.05.028.

Sezen C., Partal T., 2020, Wavelet combined innovative trend analysis for precipitation data in the Euphrates-Tigris basin, Turkey, Hydrological Sciences Journal, 65 (11), 1909-1927, DOI: 10.1080/02626667.2020.1784422.

Shah S.A., Kiran M., 2021, Mann-Kendall test: trend analysis of temperature, rainfall and discharge of Ghotki feeder canal in district Ghotki, Sindh, Pakistan, Environment & Ecosystem Science, 5 (2), 137-142, DOI: 10.26480/ees.02.2021.137.142.

Sirven P., 1987, Démographie et villes au Burkina Faso, Les Cahiers d'Outre-Mer, 40 (159), 265-283, available online at https://www.persee.fr/doc/caoum_0373-5834_1987_num_40_159_3227 (data access 07.08.2025).

Sougué M., Merz B., Sogbedji J.M., Zougmoré F., 2023, Extreme rainfall in southern Burkina Faso, West Africa: trends and links to Atlantic Sea surface temperature, Atmosphere, 14 (2), DOI: 10.3390/atmos14020284.

Sylla M.B., Giorgi F., Pal J.S., Gibba P., Kebe I., Nikiema M., 2015, Projected changes in the annual cycle of high-intensity precipitation events over West Africa for the late twenty-first century, Journal of Climate, 28 (16), 6475-6488, DOI: 10.1175/JCLI-D-14-00854.1.

Tazen F., Diarra A., Kabore R.F., Ibrahim B., Bologo/Traoré M., Traoré K., Karambiri H., 2019, Trends in flood events and their relationship to extreme rainfall in an urban area of Sahelian West Africa: The case study of Ouagadougou, Burkina Faso, Journal of Flood Risk Management, 12, DOI: 10.1111/jfr3.12507

Thomasson S.A., 2017, Improving forecast performance of LPG demand, Master's Thesis, University of Twente, 109 pp.

Trepekli K., Friborg T., Allotey A.N., Møller-Jensen L., 2019, Influence of climate change on the future precipitation pattern in the region of Ghana: Climate change resilience in urban mobility, University of Copenhagen, 16 pp.

Wiguna I.K.A.G., Utami N.L.P.A.C., Parwita W.G.S., Udayana I.P.A.E.D., Sudipa I.G.I., 2023, Rainfall forecasting using the Holt-Winters exponential smoothing method, Jurnal Info Sains: Informatika dan Sains, 13 (01), 15-23.

Yaméogo J., 2024, Changes in the seasonal cycles of extreme temperatures in the Sudano-Sahelian domain in West Africa: a case study from Burkina Faso, Meteorology Hydrology and Water Management, 12 (2), DOI: 10.26491/mhwm/194451.

Yaméogo J., 2025, Annual rainfall trends in the Burkina Faso Sahel: a comparative analysis between Mann–Kendall and innovative trend method (ITM), Discover Applied Sciences, 7, DOI: 10.1007/s42452-025-06675-1.

Yaméogo J., Rouamba S., 2023a, Extreme temperature in Burkina Faso: decadal spatio-temporal changes between 1960 and 2019, European Journal of Theoretical and Applied Sciences, 1 (6), 441-450, DOI: 10.59324/ejtas.2023.1(6).43.

Yaméogo J., Rouamba S., 2023b, Climatic disasters in Burkina Faso from 1960 to 2020: Occurrence, spatiotemporal dynamics and socio-environmental consequences, African Journal on Land Policy & Geospatial Sciences, 6 (5), 1022-1043.

Yaméogo J., Sawadogo A., 2024, Consequences of precipitation variability and socio-economic activity on surface water in the Vranso water basin (Burkina Faso), Bulletin of the Serbian Geographical Society, 104 (1), 255-266, DOI: 10.2298/GSGD2401255Y.

Yaméogo J., Yanogo I.P., Ndoutorlengar M., 2022, Approvisionnement en eau potable en milieu urbain dans les quartiers informels de la ville de Boromo (Burkina Faso): entre accommodements locaux, enjeux socioéconomiques et risques sanitaires, Annales de Moundou. Série A: Annales de la Faculté des Lettres, Arts et Sciences Humaines, 9 (1), 57-91.

Yanogo I.P., Yaméogo J., 2023, Recent rainfall trends between 1990 and 2020: contrasting characteristics between two climate zones in Burkina Faso (West Africa), Bulletin of the Serbian Geographical Society, 103 (1), 87-106, DOI: 10.2298/GSGD2301087Y.

Zhang X., Yang F., 2004, RClimDex (1.0) User Manual, Climate Research, Branch Environment, Canada, 23.